International Journal of Mechanical and Materials Engineering (IJMME), Vol. 3 (2008), No.2, 187-197.

CHARACTERIZATION OF INTERMETALLIC GROWTH OF GOLD BALL BONDS ON ALUMINUM BOND PADS

M.K.Md Arshad, Lim Moy Fung, M.N. M. Noor and U. Hashim
School of Microelectronic Engineering, Universiti Malaysia Perlis (UniMAP)
P.O Box 77, d/a Pejabat Pos Besar,01000 Kangar,Perlis, MALAYSIA
E-mail: mohd.khairuddin@unimap.edu.my

ABSTRACT

In this paper the intermetallic growth between gold ball bond and aluminum bond pad are studied. It involves thermal aging at 150 °C and 200 °C for various time intervals. The relationship between electrical resistance and intermetallic growth are investigated. Process decapsulation followed by Field Emission Scanning Electron Microscopy (FESEM) are used to determine the intermetallic coverage, intermetallic thickness and Kirkendall void of gold ball on aluminum bond pad. The quantitative Energy Dispersive X-Ray (EDX) is used to determine intermetallic phase composition. The result shows that the electrical resistance increase rapidly with temperature and time reflecting faster interdiffusion rates. The resistance might increases to infinity without degradation in bond strength. The magnitude of intermetallic growth for Au-Al increases with the increases of thermal aging and temperature. Under thermal aging, the void and separation layer propagates further and easily seen after 1000 hours and 40 hours at 150°C and 200°C respectively.

Key words: Intermetallic, Au-Al, Interdiffusion,

INTRODUCTION

In the semiconductor industry, the reliability of manufactured product is important. A minor failure in semiconductor components would lead to failure in functionality of the final electronic product. In semiconductor industry, interconnection between gold wire bonding to aluminum bond pads is accounted 90% (Harman, 1997; Baldwin, 2001) of the entire chip to package interconnection. However, these interconnections lead intermetallic formation. There are $AuAl_2$, AuAl, Au_2Al, Au_5Al_2, and Au_4Al (Philofsky, 1970) even Au_8Al_3 and Au_3Al_2 (Li *et al,* 2007) intermetallic found in the interface. Intermetallic formation is the result of the diffusion of one material into another via crystal vacancies made available by defects, contamination, impurities, grain boundaries and mechanical stress. In the Au-Al interconnection, the diffusion rate for Au in Al is different than that for Al into Au. These rates are enhanced in the function of temperature. If the material permeate the other in volume and the diffusion occurs sufficient fast, then the minority material can appear to have been completely "consumed" by the majority material. Diffusion is enabled by the movement of atoms of one material into the crystal vacancies of the other material. The vacancies will appear to be the moving feature and they can tend to coalesce and become visible in the form of voids or pores. The industry has concern with the mechanical robustness in the Au-Al interface, primarily because bare devices are exposed to temperatures in the range of 150-180 °C during moulding (inclusive of 2-3 hours post mould cure), which promotes the intermetallic growth. Then, elevated temperatures also occur from multiple high temperature excursions during board level (or other) assembly of moulded devices and from heat dissipation during device operation.

In industry, it normally use the accelerated isothermal aging tests at temperatures between 150-200 °C to stimulate rapid intermetallic growth and to test the mechanical robustness of ball bonds, by measuring the pull and shear strengths. These tests do not really assess the chemical stability of intermetallic in the presence of moulding compounds, which is an important issue (Breach et al, 2004;Uno & Tatsumi, 2000) as are thermal or thermo-chemical factors, which play a major role in the stability of intermetallic compounds. Thus, it is more beneficial to subject the samples to elevated temperatures. According to Pretorius's rules (Pretorius *et al,* 1991) several Au-Al intermetallic compounds may form, with growth and phases dictated by element availability. Exposure for about 20 hours at 175 °C, a typical 10,000 Å thick Al pad is entirely converted to an intermetallic compound (Philofsky, 1970). Many conflicting reports on intermetallic growth in ball bonds have been published (Clatterbaugh *et al,* 1984; Clatterbaugh & Charles, 990; Uno *et al*, 1992; Koeninger *et al,* 1995; Tok *et al,* 2003; Dittmer *et al,* 1998; Harman,1997), some studies reported extreme loss of mechanical strength due to reduction of contact area by the formation of voids (Clatterbaugh *et al,* 1984; Clatterbaugh & Charles, 990; Uno *et al*, 1992) and bond pad contamination (Koeninger *et al,* 1995) while other reports show good results even after extended isothermal aging at 175 °C for 1000 hours (Tok *et al,* 2003). Void formation is usually cited as being due to uneven diffusion speeds of the Au-Al atoms and the Kirkendall

effect, which has not been established as the universal mechanism for such loss of contact area occurrence. Other mechanisms, including contamination induced corrosion may explain the degradation of intermetallics (Harman, 1997; Alberici *et al,* 2003).

In this study, the primary goal is to investigate the growth of intermetallic, hence, no special corrosion affects are included during the intermetallic growth in gold ball bonds on a thin layer of Al metallization. This condition reflects the real wire bonding situation found in gold ball bonding when subjected to various thermal aging without taking into consideration of other influence mechanisms.

2.0 Experimental Procedures

Two distinct integrated circuit (IC) samples, labeled as first sample and second sample, are used in this study. A 4N type gold wire, with Au > 99.99 % and 25 µm diameter is used as the interconnection between die and lead frame using thermosonic bonding. The samples undergo a normal production process flow and procedures starting from die attach, wire bonding, molding, trim and singulation and lastly electrical testing. Once completed, the first set of samples, are subjected to high temperature storage testing (HTS) at 150 ºC for 0, 168, 500, 1000, 1500 and 2000 hour durations. The second samples set are aged at 200 °C for 0, 20, 40, 60, 70, 80 and 90 hours. The characterization starts with a resistance measurement between Drain To Source ($R_{DS(on)}$), performed with a Tektronix 371B Curve Tracer. The $R_{DS(on)}$ of the samples are taken at 0 hour as a comparison base to 168, 500, 1000, 1500 and 2000 hours for thermal aging at 150 °C; and another measurement is on the second samples at 200 °C for 20, 40, 60,70,80 and 90 hours. Since the internal circuitries for first and second sample are different, the settings for each test follow the respective datasheets. The first sample is set with a drain current, I_D = 13.2A at a gate threshold voltage, V_{GS} = 4.5V and for the second samples the drain current, I_D = 14.5A at gate threshold voltage, V_{GS} = 10V. The reason for this resistance measurement is to measure the resistivity of wire bonding.

Since the next analysis focusing on the Au-Al interface, then only the second sample is subjected to destructive analysis after the electrical measurement. Decapsulation is carried out to remove the plastic molding and expose the die area by using the B&G Jet-Etcher on the devices with 100 % fuming nitric acid at 80 °C for 25 seconds. The component is then rinsed with acetone for cleaning and followed by drying in dry air. The observation and optical imaging is performed using a Leica Microscope.

Gold ball bonds are removed by immersing the exposed dies in, 20 g Potassium Hydroxide Pellets (KOH) dissolved in 100ml deionized (DI) water for about 20 minutes, and then rinsed with DI water. Secondary electron Field Emission Scanning Electron Microscopy (FESEM) is used to capture the underside of the ball bond images. The micrograph images are then used to identify the intermetallic phase (IP) composition and coverage measurement as described (Breach & Wulff, 2004). Cross sections of the ball bonds are prepared in the normal metallographic manner, taking care not to smear the soft gold across the bond pads while ensuring that the deformation layer, caused by polishing, is minimized. Specimens are mounted onto a holder and are wet-ground with grit sizes of 600, 800, and 1200 and then follow with polishing with 0.3 and 0.05 µ grits. The intermetallic phase composition and thickness are observed using high power optical microscope and FESEM. Optical imaging is performed using Leica Microscope. A Zeiss Supra 40VP FESEM with an Oxford Instruments Inca EDX system is used for SE (Secondary Electron) and BSE (Backscattered Electron) imaging as well as Energy Dispersive X-Ray (EDX) measurements. The described process flow is illustrated in Figure 1.

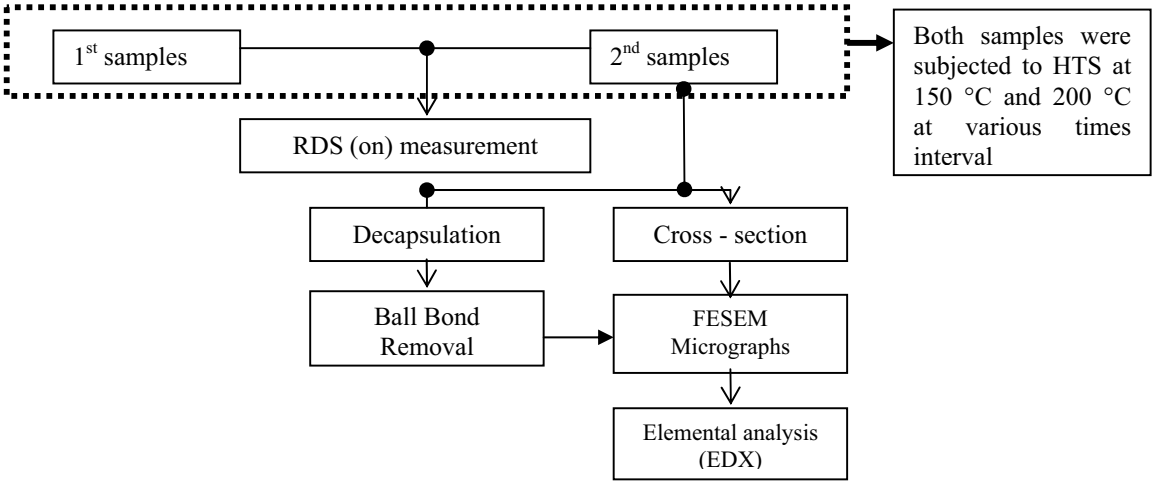

Figure 1: Experimental flow

3.0 RESULTS AND DISCUSSIONS

3.1 Static Drain To Source On Resistance ($R_{DS(on)}$) of The Sample

The resistance values as shown in Figure 2 and Figure 3 are taken after High Temperature Storage at 150 °C and 200 °C for each time intervals, described earlier respectively. It is clearly seen from Figure 2 and Figure 3 that the resistance between drain to source increased with the increasing of thermal aging time and temperature. The increased is due to increase scattering of the electrons by lattice vibrations (or phonons). Data shows no high resistance failure even after 2000 hours thermal, aging at 150 °C (as shown in Figure 2) but resistance failure is seen after 80 hours aging at 200 °C (as shown in Figure 3), at which time aging is stopped. The affect of a higher the $R_{DS(on)}$ causing a lower the signal or electrical conductivity, thus it might causes the degradation of the product output or performance.

The study shows that the electrical resistance can increase to infinity without degradation in bond strength whatsoever ((Ramsey & Alfaro, 1991). The implication is clear: problems of resistance do cause circuit failures and, which will not be detected with a bond pull or ball shear test.

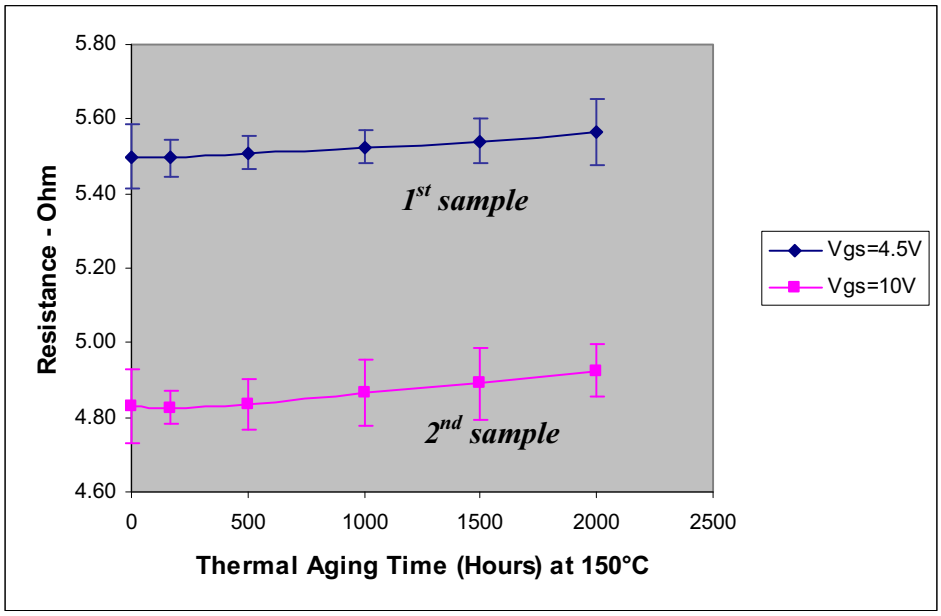

Figure 2: Drain to Source On Resistance ($R_{DS(on)}$) after thermal aging time at 150 °C

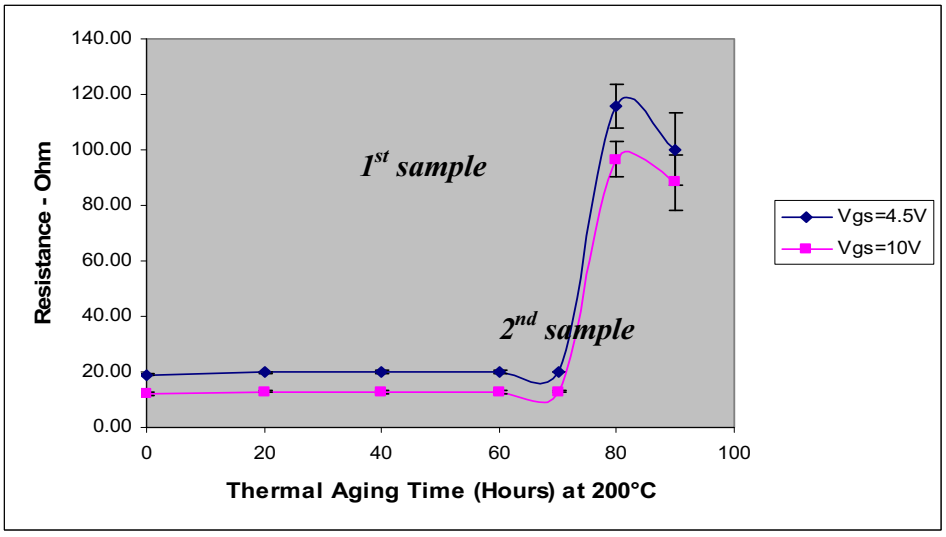

Figure 3: Drain to Source On Resistance ($R_{DS(on)}$) after thermal aging time at 200 °C

3.2 Intermetallic Coverage of Au ball bonds on The Al Bond Pad

Figure 5 (a) to (f) depicts the intermetallic coverage of the ball bond as seen from micrograph images at the bottom of the bonded ball after aluminum metallization has been etched. This is done after the sample is subjected to different thermal aging intervals at 150 °C.

At zero hour condition, the regions of the unbonded ball demonstrates that the transfer of ultrasound from the capillary to the Au ball bond to Al bond pad interface is not uniform, which is a characteristic of the thermosonic ball bonding process. The intermetallic coverage obtained with a typical initial-bonded Au ball bond is very defined and clearly visible as shown in Figure 5(a).

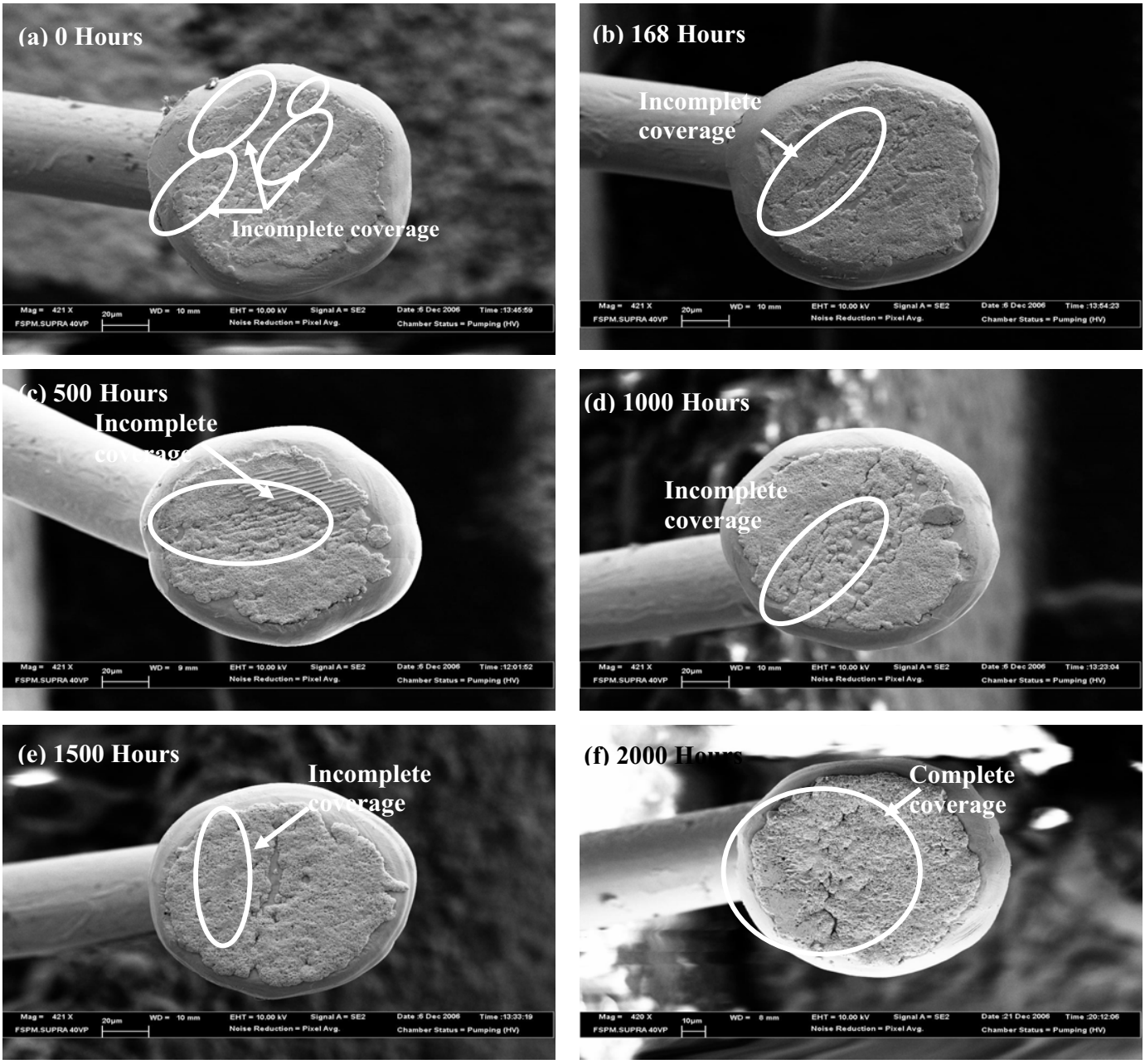

Figure 5: Micrograph image shows the intermetallic coverage of thermal aging at 150 °C for (a) 0 hour, (b) 168 hours, (c) 500 hours, (d) 1000 hours, (e) 1500 hours, and (f) 2000 hours

The relatively small but irregular surface morphology area of the intermetallic phase that has grown with assistance from the ultrasonic bonding and the growth is then further enhanced, during thermal aging tests, as seen in Figure 5 (b) to (f), where less irregularities is surface morphology are seen. The growth (intermetallic coverage and thickness) has increased over the exposure times due to interdiffusion between Au and Al occurring continually. After thermal aging at 200 °C as shown in Figure 6, the intermetallic coverage at zero hour condition is similar to that seen in devices aged at 150 °C. However, the intermetallic coverage is more uniform and seen has growth thicker after 20 hours (Figure 6(b)) of thermal aging compare to that at 150 °C (Figure 5(b) to (e)). This occurrence is due to the high diffusion rate between Al and Au. After 40 hours thermal aging, it clearly seen the bond pad aluminum stuck on the underside of the gold ball as shown in Figure 6 (c) to (d). This occurrence is due to the high diffusion rate between Al and Au causing the Al to be completely consumed by the intermetallic phase. At 80 hours, as shown in Figure 6 (f), no Al is observed because the intermetallic has completely consumed the aluminum bond pad resulting in a lifted ball failure.

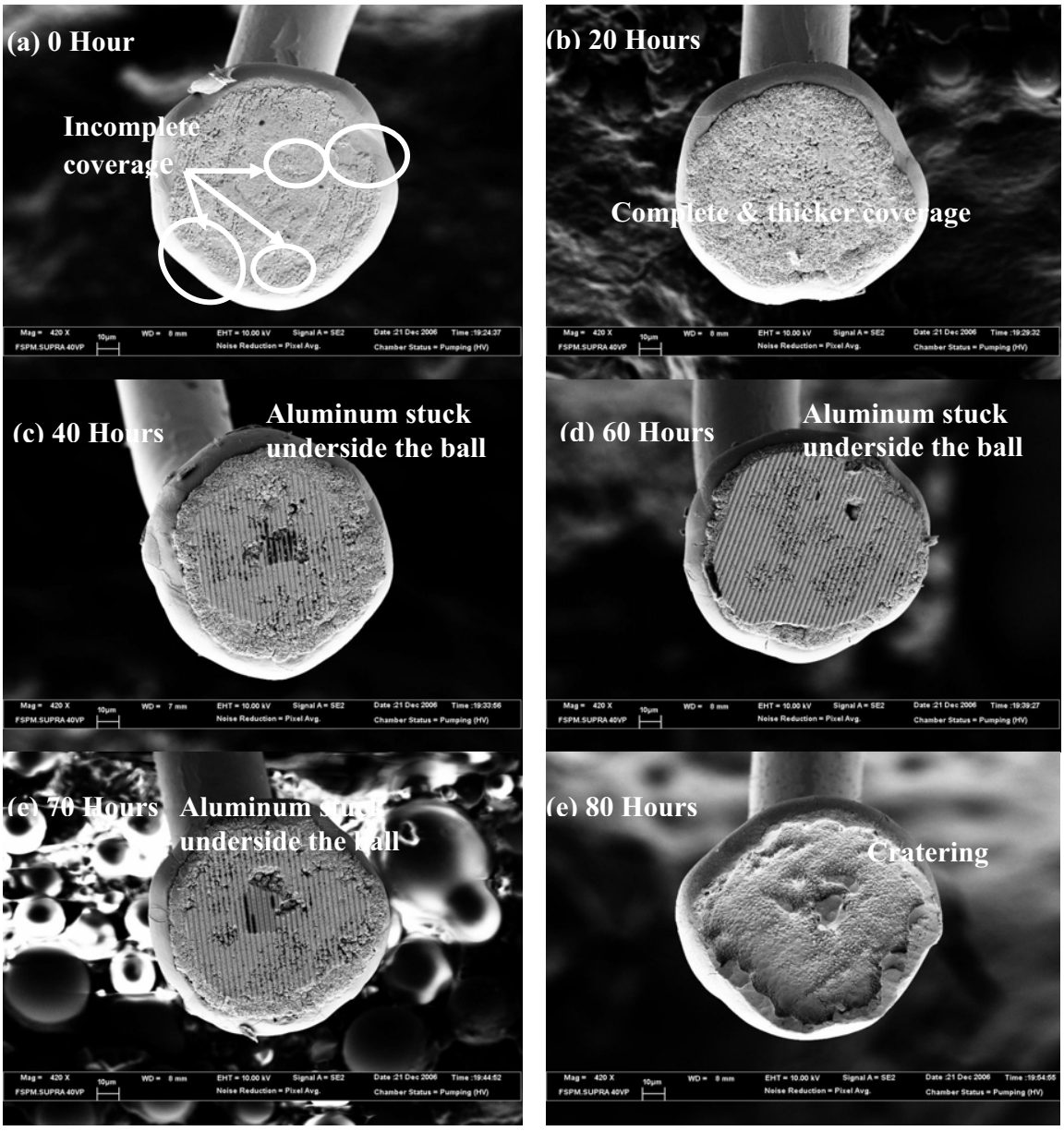

Figure 6: Micrograph image shows the intermetallic coverage of aged samples at 200 °C for (a) 0 hour, (b) 20 hours, (c) 40 hours, (d) 60 hours, (e) 70 hours, and (f) 80 hours

3.3 Intermetallic Growth and Kirkendall Voiding

Figure 7 and Figure 8 show cross-sections of the ball bond after various exposure times and thermal aging. The growth rates of Au-Al intermetallic at 200 °C is faster compared to 150 °C across various aging times. The as-bonded balls specimen in Figure 7 (a) and Figure 8 (a) show the initial intermetallic as discrete small islands across the diameter of the ball, reflecting a coverage pattern as in Figure 5 (a) and Figure 6 (a) of which the unbonded areas are clearly visible. After exposure to thermal aging at 150 °C for 168 hours (Figure 7(b)), the intermetallics start to grow vertically and laterally at the interface but in slower rates.

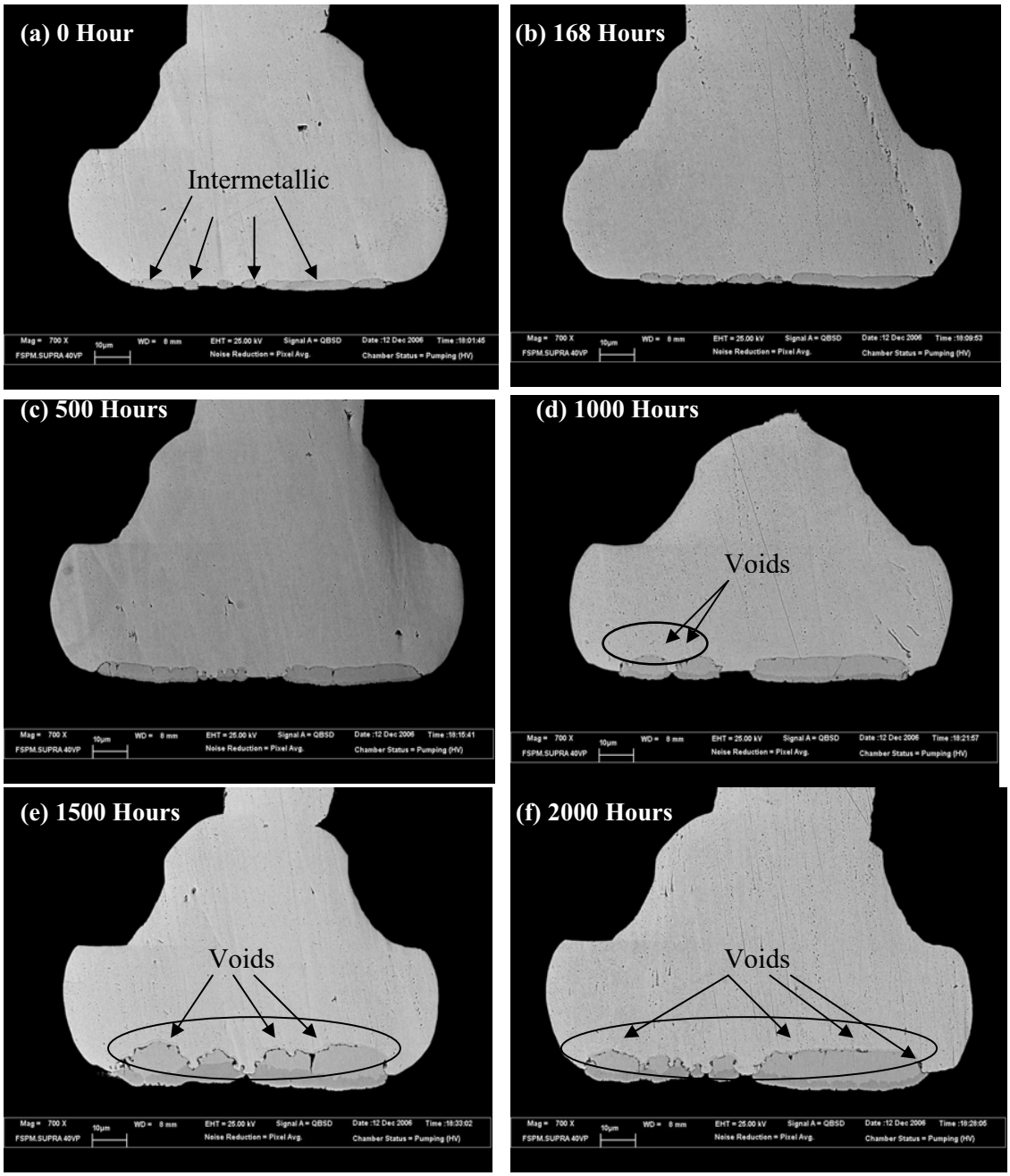

Figure 7: Micrograph image shows the intermetallic phase of aged samples at 150 °C for (a) 0 hour, (b) 168 hours, (c) 500 hours, (d) 1000 hours, (e) 1500 hours, (f) 2000 hours.

In Figure 7 (c) to (f) show that in between 500 - 2000 hours, there are increased in thickness of total intermetallic phase. At 500 hours, the void formation is believed to have started to grow within of the Au-intermetallic interface. The intermetallic and void growth is confined to the contact zone of the ball. After 1000 hours, the voids formations are appeared. At 1500 hours and 2000 hours, the voids formation continues and clearly seen, while intermetallic still growing but at slower rate.

Figure 8 (b) shows rapid intermetallic growth at the interfaces after 20 hours of exposure at 200 °C. It consumes the Al pad, and the intermetallic growth slows down and stabilizes after 40 - 60 hours because interdiffusion between Au and Al is almost complete. The voids are seen at this stage.

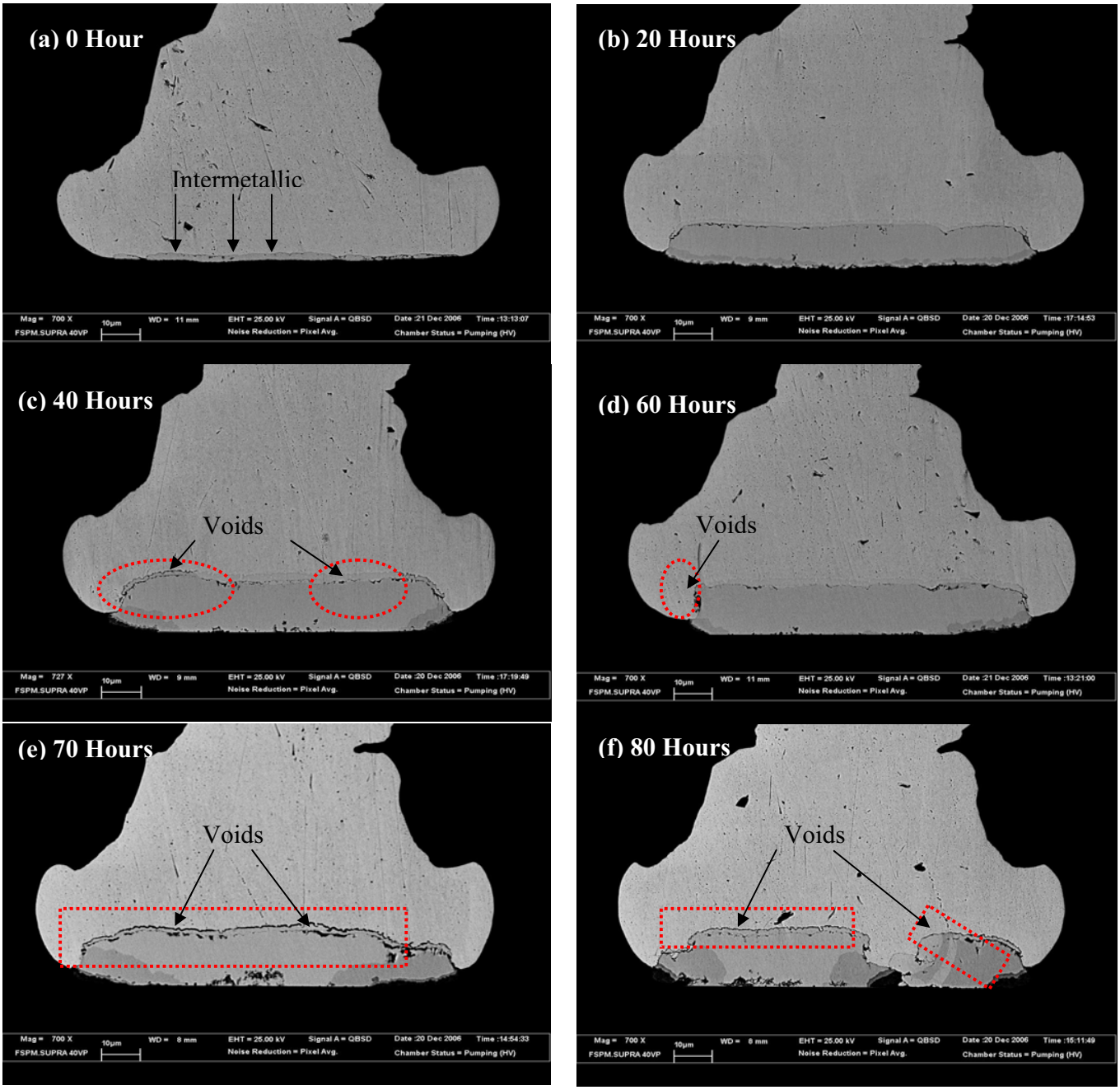

Figure 8: Micrograph image shows the intermetallic phase of aged samples at 200 °C for (a) 0 hour, (b) 20 hours, (c) 40 hours, (d) 60 hours, (e) 70 hours, (f) 80 hours.

At 70 and 80 hours, the void continues to form, while intermetallic growth has stopped due to interdiffusion reaction between Au and Al and the voids are clearly visible in between two intermetallic layers as shown in Figure 8 (e) – (f). From the results in Figure 7 and Figure 8, the thickness of the intermetallic layer is extracted and plotted as shown in Figure 9. It is suspected that the Al metallization is completely consumed after 80 hours at 200 °C, while the interdiffusion still occur even after 2000 hours for 150 °C. The intermetallic thickness increase because the intermetallic compound continues to form resulted from interdiffusion.

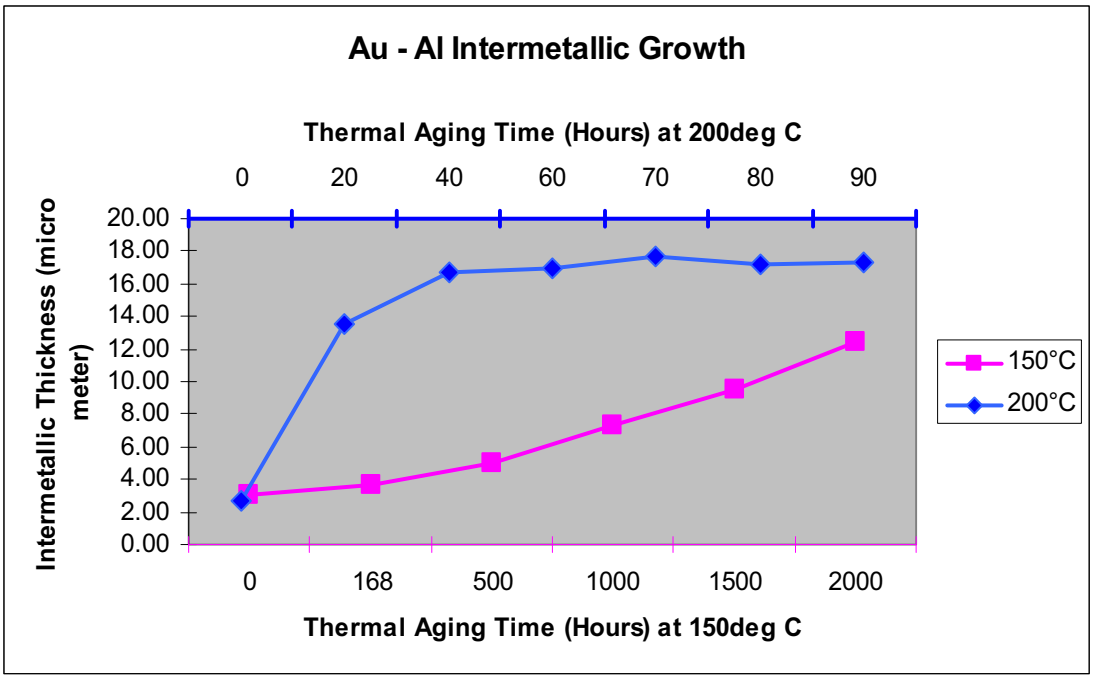

Figure 9: Intermetallic growth at 150 °C and 200 °C for various thermal aging times

3.4 Intermetallic Phases and Kirkendall Voiding

Figure 10 depicts the micrograph images of cross-sectioned ball bonds from the as-bonded condition up to 2000 hours at 150 °C. The quantitative EDX-FESEM reveals three phases for samples up to 1500 hours as shown in Figure 10 (a) – (f). It consists of upper thin (Au_4Al), middle (Au_5Al_2) and lower grained phase (Au_5Al_2) and at 2000 hours it has an additional bottom lower (Au_2Al) phase near the chip. The voids are visible between the Au_5Al_2 phase and Au_4Al, presumably due to uneven diffusion across the phase boundaries during growth. The void is then extended into the middle grained phase. This result shows that between 168 - 1500 hours, Au_5Al_2 is the dominant phase with Au_4Al present as a very thin layer and another Au_5Al_2 layer at the bottom. At 2000 hours, quantitative EDX analysis shows the presence layers of a thin layer of Au_2Al phase near the chip as shown in Figure 9 (f). However, the Au_4Al could also remain as a thin layer next to the ball while the Au_5Al_2 phase is dominant. Figure 11 indicates the micrograph image of cross-sectioned ball bonds from the as-bonded condition up to 80 hours at 200 °C. Similar to thermal condition at 150 °C, the micrograph image reveals three phases that initially appeared as result shown in the Figure 11 (a) to (f). It consists of upper thin (Au_4Al), middle (Au_5Al_2) and lower grained phase (Au_5Al_2) and after above 1500 hours (Figure (e) to (f)) it has an additional bottom lower (Au_2Al) phase near the chip. After 20 hours thermal aging, quantitative EDX shows two layers of Au_4Al presence, with a thicker coarse-grained phase and thin fine-grained phase presence adjacent to the Au_5Al_2 phase near the chip. From the limited amount of information available on these phases as mentioned by Hansen (1958), the α-Au_4Al is polymorphic and exist in two form – cubic and rhombohedral (Uno *et al,* 1990). The observations show that the voids occur between the two types of Au_4Al. At 40 hours and 60 hours, the thickness of Au_4Al at the upper layer has not much increases as compared with lower layer of Au_4Al which almost consumed the Au_5Al_2, i.e. the Au_5Al_2 phase is transforming to Au_4Al. After 70 hours and 80 hours, the thin layer of Au_2Al presence because of continuous diffusion of Al into gold

ball during thermal aging. Finally, the layer of $AuAl_2$ also presence and lifted ball occurred when a coarse grained and thicker $AuAl_2$ phase was formed as shown in Figure 11 (e) and (f). From the result shown in Figure 10 and Figure 11, it clearly seen that the interdiffusion between Au-Al at thermal condition 200 °C is faster than at 150 °C. Identification of the phases and the sequences of phase formation in gold ball bonds can aid interpretation of failure modes after thermal aging testing. However, many reports (Clatterbaugh *et al,* 1984; Clatterbaugh & Charles, 990; Uno *et al*, 1992) on intermetallic growth in gold ball bonds that are not in agreement on the sequences or the final phases that remains after extended aging times.

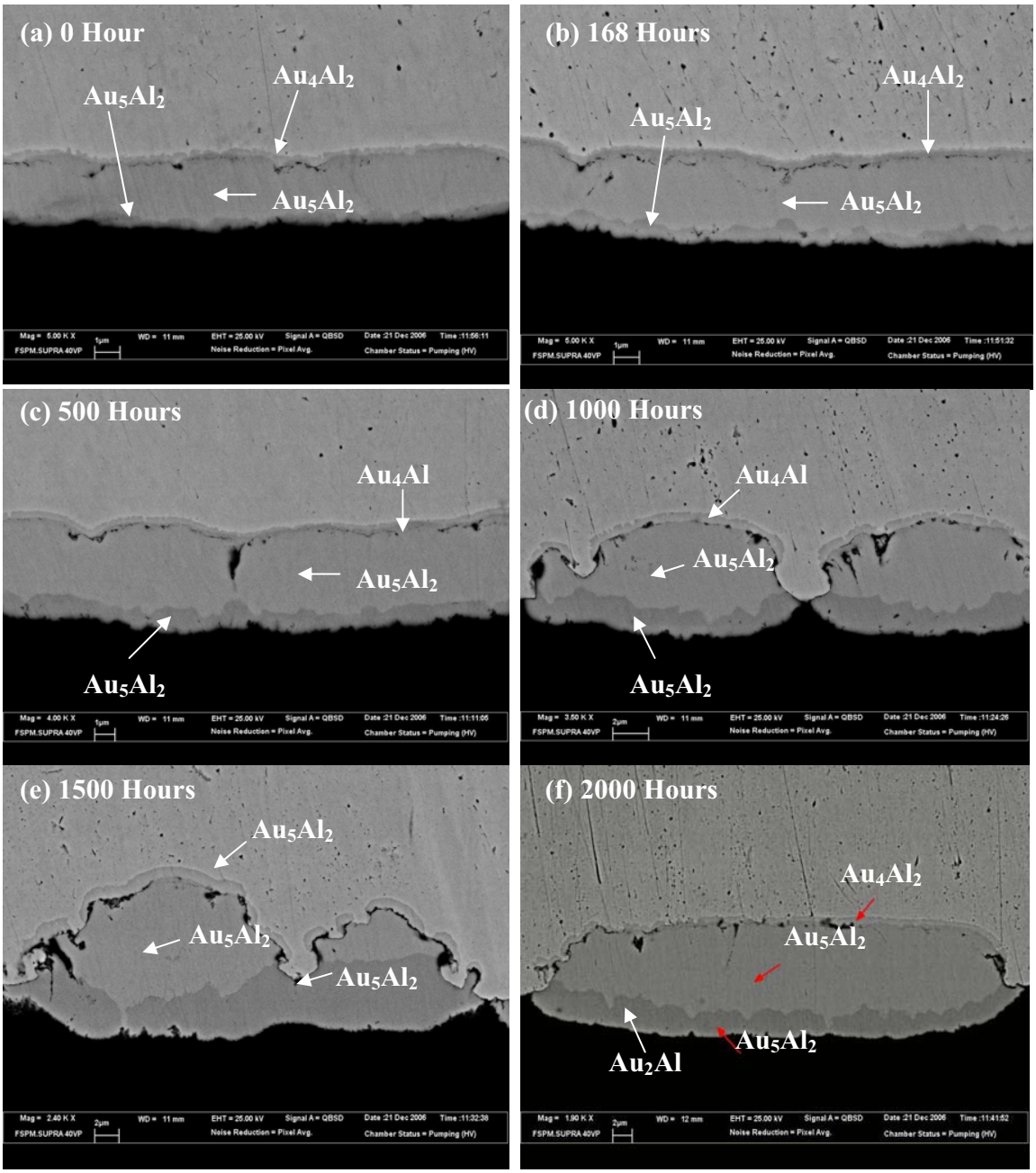

Figure 10: Micrograph image shows the intermetallic phase of aged samples at 150 °C for (a) 0 hour, (b) 168 hours, (c) 500 hours, (d) 1000 hours, (e) 1500 hours, (f) 2000 hours.

They have recognized that bonding conditions affect the result of thermal aging test. There is, however, good evidence that Au_5Al_2 is the first phase to form and grow rapidly. This is an agreement result in Figure 10 and Figure 11, the Au_5Al_2 is the dominant phase as-bonded condition, the Au_4Al and Au_5Al_2 are both presence after 168 hours at 150 °C and 20 hours at 200 °C. Quantitative EDX result shows that after 20 hours aging at 200 °C, Au_4Al is the dominant phase at the ball center, with Au_5Al_2 at the lower region, close to chip. The Au_4Al phase, initially formed at the ball center, is also observed to consume the Au_5Al_2 at the ball periphery. From various reports (Clatterbaugh *et al,* 1984; Clatterbaugh & Charles, 990; Uno *et al*, 1992), the thin layer could be Au_2Al due to its higher heat of formation. The Au_2Al is formed, probably because a smaller supply of gold at the peripheral region forces the transformation of Au_5Al_2 – Au_2Al. However the Au_8Al3 and Au_3Al_2 as mentioned (Li *et al*, 2007) could not be verified.

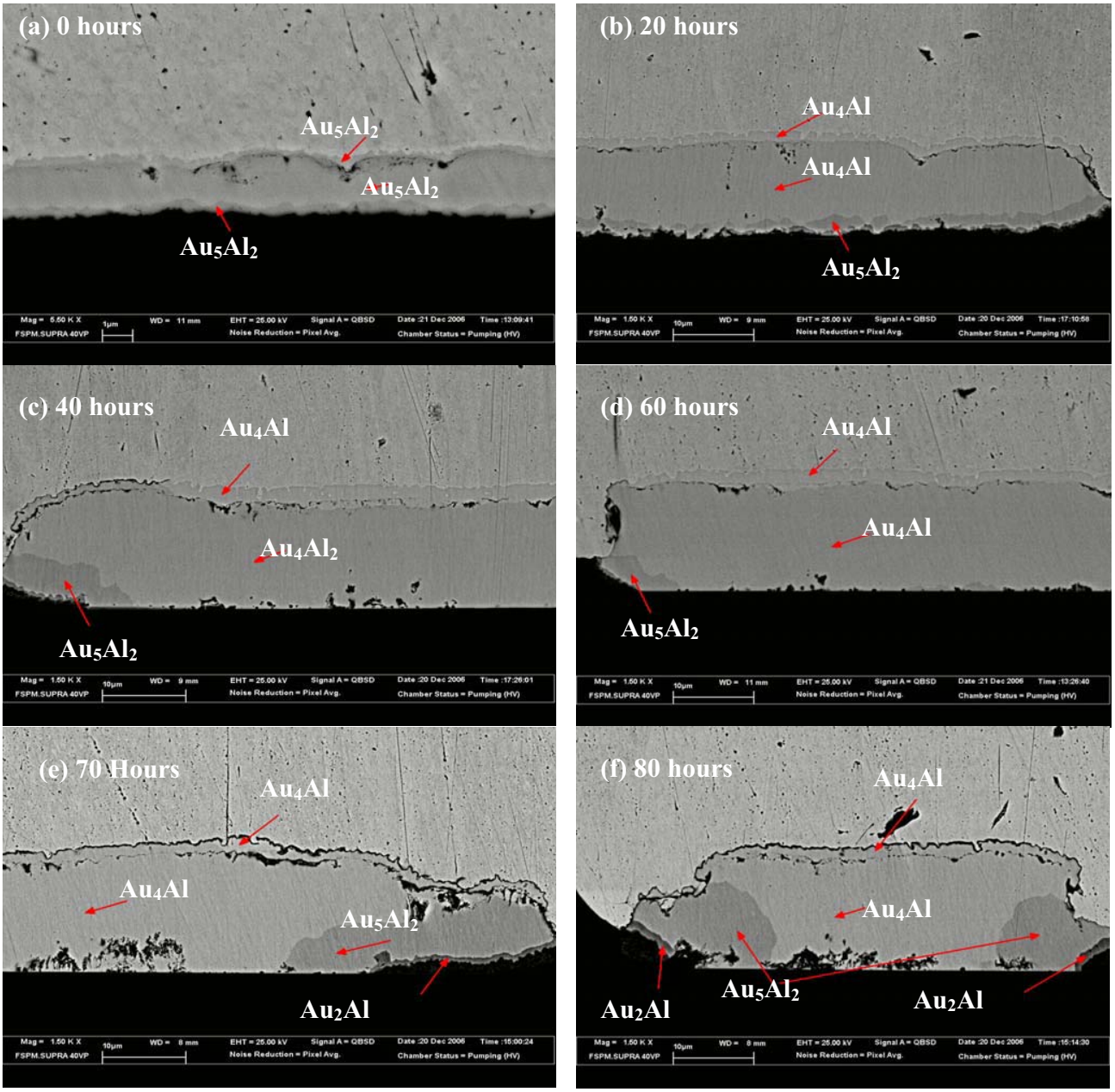

Figure 11: Micrograph image shows the intermetallic phase of aged samples at 200 °C for (a) 0 hour, (b) 20 hours, (c) 40 hours, (d) 60 hours, (e) 70 hours, (f) 80 hours.

4.0 CONCLUSION

There are five intermetallic exist in the Au-Al system are presence in equilibrium at any given temperature - $AuAl_2$, AuAl, Au_2Al, Au_5Al_2, and Au_4Al. Intermetallics grow continuously; the quantity of Au and Al available determines the type, amount, and sequences of intermetallic formed. The electrical resistance increase rapidly with temperature and it might increase to infinity without degradation in bond strength. The implication is clear: problems of resistance do cause circuit failures and, which will not be detected with a bond pull or ball shear test.

That is no high resistance failure even after 2000 hours aging at 150 °C but resistance failure is seen after 80 hours aging at 200 °C. At 200 °C thermal aging, the growth rate of Au-Al phases is faster compare to thermal aging at 150 °C. The morphology of Au-Al intermetallic compound grow laterally, vertically and rapidly during thermal aging at 200 °C compare with intermetallic formed at 150 °C. At 150 °C thermal aging, Kirkendall voiding begins at the interface between Au_5Al_2 and Au_4Al At 200 °C thermal aging, two Au_4Al compounds are formed by phase transformation of the Au_5Al_2 after longer aging time and Kirkendall voiding are appear between two Au_4Al compounds. The kirkendall voiding results is due to unequal diffusion rates between the gold-aluminum especially Au_5Al_2 and Au_4Al phases.

5.0 REFERENCES

Alberici, S., Coulon, D., Joubin, P., Mignot, Y., Oggioni, L., Petruzza, P., Pium, D. and Zanott, L. 2003. Surface Treatment of Wire Bonding Metal Pads, Microelectronic Engineering, Vol. 70, pp. 558-565

Baldwin, D.F. 2001. Fundamentals of Microsystems Packaging, McGraw Hill, New York.

Breach, C.D., Wulff, F., Dittmer, K, Garnier, M, Boillot, V., Tok, C.W. 2004. Reliability and Failure Analysis of Gold Ball Bonds in Fine and Ultra-fine Pitch Applications. Proceedings of Semicon Technical Symposium S2, pp. 78-87

Breach, C. D. and Wulff, F. 2004. New Observation on Intermetallic Compound Formation in Gold Ball Bonds: General Growth Patterns and Identification of Two Forms of Au4Al. Microelectronics Reliability, Vol. 44, pp. 973-981.

Clatterbaugh, G.V., Weiner, J.A. and Charles, H.K. 1984. Gold-Aluminum Intermetallics: Ball Bond Shear Testing and Thin Film Reaction Couples. IEEE Trans. Comp., Hybrids and Manufacturing Technolog, Vol. 7, pp. 349-356.

Clatterbaugh, G.V., and Charles, H.K. 1990. The Effect of High Temperature Intermetallic Growth on Ball Shear Induced Cratering. IEEE Trans. Comp., Hybrids and Manfg., Vol. 13, pp. 167-171.

Koeninger, *et al.* 1995. Degradation of Gold-Aluminum Ball Bonds by Aging and Contamination, IEEE Trans. on CPMT, Part A, Vol. 18, pp. 835-841.

Li, H., Li, M., Wang, C., Bang, H.S. 2007. Comparison of Interface Evolution of Ultrasonic Aluminum and Gold Wire Wedge Bonds During Thermal Aging. Material Science & Engineering A.Vol. 447, pp. 111- 118.

Dittmer, K., Kumar, S. and Wulff, F. 1998. Intermetallic Growth in Small Gold Bonds, Proc. SEMICOM Singapore, Test, Assembly & Packaging, pp.267-272.

Hansen, M. 1958. The Constitution of Binary Phase Diagrams, 2d Ed., McGraw-Hill, New York.

Harman, G. G. 1997. *Wire Bonding in Microelectronics*, 2d Ed., McGraw-Hill, New York.

Philofsky, E. 1970. Intermetalic Formation in Gold-Aluminum System, Solid State Electronics, Vol. 13, pp. 1391-1399

Pretorius. R., Vredenburg, A.M., Saris F. W. and de Reus R. 1991. Prediction of phase Formation Sequence and phase Stability in Binary Metal-aluminum thin film systems using the effective heat of formation rule, J. Appl. Phys, Vol. 70, pp.3636-3642

Ramsey, T.H. and Alfaro, C. 1991. The Effect of Ultrasonic Frequency on Intermetallic Reactivity of Au-Al Bonds, Solid State Technology, Vol. 34, pp.37-38.

Tok, C. W., Dittmer, K., Breach, C.D. and Wulff, F. 2003. Comparison of 2N and 4N Gold Bumping Wire, Proceedings of Semicon Singapore Technical Symposium (STS) Adv. Packaging Tech. II, pp. 19-24.

Uno T, Tatsumi K and Ohno Y. 1992. Void Formation and Reliability in Gold-Aluminum Bonding. Proc. ASME/JSME Advances in Electr. Packaging EEP, Vol. 1-2.

Uno T and Tatsumi K. 2000. Thermal reliability of Gold-Aluminum Bonds Encapsulated in Bi-phenyl Epoxy Resin, Microelectronics Reliability, Vol. 40, pp. 145-151.